ELSEVIER

Chemical Engineering Journal 81 (2001) 261–269

Chemical Engineering Journal

www.elsevier.com/locate/cej

Computational modeling of pulverized coal combustion processes in tangentially fired furnaces

Jianren Fan*, Ligeng Qian, Yinliang Ma, Ping Sun, Kefa Cen

Department of Energy Engineering, Zhejiang University, Hangzhou 310027, PR China

Received 9 December 1998; received in revised form 18 April 2000; accepted 2 May 2000

Abstract

In this work, an Eulerian/Lagrangian approach has been employed to investigate numerically flow characteristics, heat transfer and combustion processes in a tangentially fired furnace. A new method of cell face velocity interpolation for non-staggered grid system is employed to avoid pressure oscillation. Grid-independence tests have been conducted. To avoid pseudo-diffusion that is significant in modeling tangentially fired furnaces, some attempts have been made at improving the finite-difference scheme. The standard k-ε model performs well in predicting flows without swirling or without sharp change within the calculated region. But for tangentially fired boiler furnaces, where swirling flow is very marked, we must resort to other more valid, more efficient turbulent models to gain accuracy. In this paper, we try to use RNG k-ε model as an alternative to the standard k-ε model. Comparisons have been made between standard k-ε and RNG k-ε models. Some new developments on turbulent diffusion of particles are taken into account for improving computational accuracy, and probability error is also discussed. Finally, temperature deviation is studied numerically so as to gain deeper insight into tangentially fired furnaces.

Keywords: Non-staggered grid; Artificial viscosity method; RNG k-ε model; Particle dispersion; Temperature deviation

1. Introduction

There are large amounts of anthracite and lean coal in China, which provide part of the generated electricity. At present, tangentially fired boilers are widely used to burn anthracites and low-volatile-matter coals. Problems such as dealing with large amounts of combustible matter in fly ash, combustion instabilities at low loads, temperature deviation of super-heaters and re-heaters, slagging in furnaces have not yet been solved. Numerical computation is known to be an efficient and promising way to provide information both in boiler design and operation, and there has been a wide coverage of literature in this field [1–3]. However, power plant research is based on complicated phenomena that involve complex physical and chemical processes that need to be modeled as precisely as possible. Despite the remarkable progress shown in the literature, there are still significant remaining questions that necessitate further research. Generally, simulations of power plant boilers include several indispensable parts: turbulent flow and turbulent transfer processes, coal-particle motion and turbulent diffusion, turbulent combustion, evaporation devolatilization and carbon combustion, heat transfer between gas particles and the walls of furnaces. Comprehensive models of combustion processes have been the subject of many investigations. These comprehensive models are based on the numerical solution of multidimensional differential equations for conservation of mass, energy and momentum, combined with rate-processes laws of correlation, physical and chemical properties, and coefficients from experimental data. In this work, we focus on improving numerical accuracy by using newly developed non-staggered grid technology, introducing a highly accurate, highly stable finite-difference scheme and incorporating an updated k-ε model into the flow field simulation. We also introduce a new stochastic dispersion model for particle tracing and discuss industrial concerns of temperature deviation. The data resulting from the present study may be used to enhance the understanding of combustion processes and also provide a useful basis for further researching comprehensive models of combustion processes and designing and operating boiler furnaces with high-efficiency.

2. Global mathematical models

In this work, a Lagrangian/Eulerian approach has been employed for gas–solid two-phase flow simulation. The gas

* Corresponding author. Fax: +86-571-799-1863.
E-mail address: fanjr@mail.hz.zj.cn (J. Fan).

1385-8947/01/$ – see front matter
PII: S1385-8947(00)00212-6

Nomenclature

A	coefficient in numerical equation
A_p	coal-particle area
c	specific heat
C_E	coefficient in EBU model
C_g	gas molar concentration
C_P	specific heat
d	particle diameter
D_w	binary diffusivity
E	activation energy
$E(K)$	energy spectrum
f	source term excluding pressure gradient
F	force
g	gravitational acceleration
h	enthalpy
k	turbulent kinetic energy
K	wave number
m	mass
M	molecular weight
Nu	Nusselt number
p	pressure
Q	heat energy
r	particle reaction rate
r_h	the carbon reaction rate
r_{hl}	the char oxidizing rate
r_p	total reaction rate for the coal particle
R	thermodynamics constant
R_1	random number
R_2	random number
Re	Reynolds number
S	source term
t	time
T	temperature
u	velocity along x direction
u_f	the instantaneous gas phase velocity
u'_f	the fluctuation gas phase velocity
u'_g	the fluctuation velocity in an eddy
U_f	the average gas phase velocity
U_m	the fluctuation amplitude
$\bar{v}$	artificial viscosity
v	velocity along y direction
V	cell volume
V	averaged velocity
V_{daf}	volatile matter from coal dust
w	velocity along z direction
W	reactive rate
x	coordinate
X	mole fraction
y	coordinate
Y	concentration
z	coordinate

Greek letters

α	initial fluctuating phase
δ	control volume width
ε	turbulent dissipation
γ	energy diffusion
λ	conducting coefficient
μ	viscosity
ρ	density
σ	Stefan–Boltzman constant
ϕ	general variables

Subscripts

C	convection
daf	Daf coal
h	char-oxidation
r	radiation
V	devolatilization
W	evaporation

phase is described by the Navier–Stokes equations, coupled with appropriate equations for density and viscosity. For closure of the turbulence equations, we use both a k-ε model and a RNG k-ε model, then make a comparison between them. The general Eulerian equation for the gas phase takes the form

$$\mathrm{div}(\rho v\phi) - \mathrm{div}(\Gamma \mathrm{grad}\,\phi) = S_\phi \tag{1}$$

where S_ϕ is the source terms of the gas phase, and Γ_ϕ the effective viscosity that is summarized in Table 1 for the different variable ϕ; where ϕ represents the variables u, v, w, k and ε (coordinate velocities, turbulent fluctuation energy and turbulent energy dissipation) [4].

A modified SIMPLER method [5] has been employed to determine velocities and pressures using a non-staggered grid system in Cartesian coordinates as demonstrated in the following part.

The heat transfer equation is

$$\begin{aligned}(\rho u C_P T)\,\Delta y\,\Delta z + (\rho v C_P T)\,\Delta x\,\Delta z + (\rho w C_P T)\,\Delta x\,\Delta y \\ = \lambda_x T\,\Delta y\,\Delta z + \lambda_y T\,\Delta y\,\Delta z + \lambda_z T\,\Delta y\,\Delta z + Q_{\text{radiation}} \\ -4K_\varepsilon \sigma T^4\,\Delta V + Q_{\text{reaction}}\,\Delta V\end{aligned} \tag{2}$$

where, ρ is the density, λ the conducting coefficient, σ the Stefan–Boltzman constant, T the temperature, C_P the specific heat, u, v and w the velocities, $Q_{\text{radiation}}$ the radiation energy transfer, which is modeled by using Monte Carlo method, and Q_{reaction} is the heat energy released during coal combustion, which is modeled as a source term after completing particle tracing.

The equation of motion for a particle is

$$\begin{aligned}m_p\left(\frac{\mathrm{d}\vec{v}_p}{\mathrm{d}t}\right) = m_p\vec{g} + \tfrac{1}{2}\rho C_D(\vec{v}_g - \vec{v}_p)|\vec{v}_g - \vec{v}_p|A_p \\ + \vec{F}_{\text{reaction}}\end{aligned} \tag{3}$$

where $\vec{F}_{\text{reaction}} = \vec{V}_J(-m_{vp}/\mathrm{d}t)$ is the force exerted on the coal particle due to sudden momentum change when devolatilization occurs, the direction of the reaction force is

Table 1
Eulerian conservation equations and identification of terms in Eq. (1)[a]

ϕ	Γ	S_ϕ
1	0	0
u	μ_{eff}	$-\frac{\partial p}{\partial x}+\frac{\partial}{\partial x}\left(\mu_{\text{eff}}\frac{\partial u}{\partial x}\right)+\frac{\partial}{\partial y}\left(\mu_{\text{eff}}\frac{\partial v}{\partial x}\right)+\frac{\partial}{\partial z}\left(\mu_{\text{eff}}\frac{\partial w}{\partial x}\right)$
v	μ_{eff}	$-\frac{\partial p}{\partial y}+\frac{\partial}{\partial x}\left(\mu_{\text{eff}}\frac{\partial u}{\partial y}\right)+\frac{\partial}{\partial y}\left(\mu_{\text{eff}}\frac{\partial v}{\partial y}\right)+\frac{\partial}{\partial z}\left(\mu_{\text{eff}}\frac{\partial w}{\partial y}\right)$
w	μ_{eff}	$-\frac{\partial p}{\partial z}+\frac{\partial}{\partial x}\left(\mu_{\text{eff}}\frac{\partial u}{\partial z}\right)+\frac{\partial}{\partial y}\left(\mu_{\text{eff}}\frac{\partial v}{\partial z}\right)+\frac{\partial}{\partial z}\left(\mu_{\text{eff}}\frac{\partial w}{\partial z}\right)$
k	$\mu_{\text{eff}}/\sigma_k$	$G_k-\rho\varepsilon$
ε	$\mu_{\text{eff}}/\sigma_\varepsilon$	$\frac{\varepsilon}{k}(C_1G_k-C_2\varepsilon)$

[a] $G_k=\mu_{\text{eff}}\left\{2\left[\left(\frac{\partial u}{\partial x}\right)^2+\left(\frac{\partial v}{\partial y}\right)^2+\left(\frac{\partial w}{\partial z}\right)^2\right]+\left(\frac{\partial u}{\partial y}+\frac{\partial v}{\partial x}\right)^2+\left(\frac{\partial v}{\partial z}+\frac{\partial w}{\partial y}\right)^2+\left(\frac{\partial w}{\partial x}+\frac{\partial u}{\partial z}\right)^2\right\}$, $\mu_{\text{eff}}=\mu_t+\mu$, $\mu_t=C_\mu\rho k^2/\varepsilon$, $C_\mu=0.09$, $C_1=1.44$, $C_2=1.92$, $\sigma_k=1.0$, $\sigma_\varepsilon=1.3$.

modeled stochastically, compared to drag force this force is smaller in quantity but important for particle trajectory. When the particle has advanced in the furnace, reaction processes like vaporization, devolatilization and char combustion should be taken into consideration.

Diffusion-limited vaporization of moisture from the coal particle is described by Fu et al. [6]:

$$r_w = M_w\, Nu_m\, C_g D_{wm} A_p \left(\frac{(X_{wp}-X_{wg})}{d_p(1-X_{wp}r_p/r_w)}\right) \tag{4}$$

Fu et al. used the equations

$$\frac{dV}{dt} = (V'_{daf}-V)K\exp\left(\frac{E}{RT}\right), \tag{5}$$

$$V'_{daf} = QV_{daf}, \tag{6}$$

to describe the formation of volatile matter from coal dust. Char is produced in competition with volatile production as expressed by

$$r_{hm} = r_v\frac{(1-Y_m)}{Y_m}. \tag{7}$$

Char assumes to be oxidized heterogeneously by a gaseous oxidizer that diffuses to the particle, is absorbed, reacts with carbon, and is then described as CO. The char-oxidizing rate is

$$r_{hl} = \frac{(A_p n_p)^2 M_{hp} m_g \phi_l K_{pl}\xi_p C_{og} C_g}{[M_g A_p n_p C_g(\xi_p K_{pl}+K_{cpl})+r_p]}. \tag{8}$$

The total reaction rate for the coal particle is

$$r_p = r_v + r_{hl} + r_w. \tag{9}$$

The carbon reaction rate is

$$r_h = r_{hm} - r_{hl}. \tag{10}$$

The mass change of a particle follows

$$\frac{dm_p}{dt} = m_w + m_V + m_h \tag{11}$$

where m_w, m_V and m_h are the rate of mass change when the coal particle is evaporated, devolatilized and char-oxidized, respectively.

The conservation of particle energy is

$$m_p\left(\frac{dh_p}{dt}\right) = Q_c + Q_r + Q_w + Q_V + Q_h \tag{12}$$

where Q_c, Q_r, Q_w, Q_V and Q_h are referring to heat related to gas-particle convection, radiation and heat release during evaporation, devolatilization and char-oxidation along the trajectory of the particle.

The EBU-Arrhenius model models gas phase turbulent combustion process:

$$W_{fu} = \min(W_{fu,A}, W_{fu,T})$$

$$W_{fu,A} = A\rho Y_{fu} Y_{O_2}\exp\left(\frac{-E}{RT}\right)$$

$$W_{fu,T} = \rho\min(Y_{fu}, Y_{O_2})C_E\frac{\varepsilon}{R} \tag{13}$$

Equations with the form of $dx/dt=f(x,t)$ are integrated using a five-stage Runge–Kutta method as described in [7].

3. Some specific concerns

3.1. Artificial viscosity method

How to reduce pseudo-diffusion in numerical simulation has been a long time concern in furnace simulations, especially in tangentially fired boiler furnaces. One way to reduce pseudo-diffusion is to adopt an adjustable grid system to keep inlet jet direction as parallel to x- or y-coordinate as possible [8]. In this work, we focus on an improved finite-difference method. Here we attempt to compare the exponential scheme with the artificial viscosity method [9].

The discussions on the effect of two schemes are included in Section 5.

3.2. Non-staggered grid system and boundary conditions

The numerical procedure for gas phase flow is based on a well known volume finite discretization of non-staggered grids. A five-stage iteration method is used in integrating the conventional difference motion equations of coal particle [10]. The simulations are carried out using a grid comprising $35\times37\times143$ control volumes. Grid-independence tests are conducted; the results are included in Section 5. The specified grid is fine enough to give grid-independent solutions. Since the numerical code solves the elliptic form of the differential equations, information about the boundary conditions surrounding the domain of interest is required. (i) Wall friction is supplied only to the gas. The usual non-slip conditions apply at the furnace wall. To account for the furnace-wall effect in the nearby regions, equations are introduced to link velocities. Due to the application of RNG k-ε, we are exempted from the trouble of introduction of the wall function in the near-wall region. (ii) Heat transfer to the wall occurs through a prescribed heat sink via the gas. Empirical expressions exist for particle-to-wall heat transfer [11]. (iii) Finally, a constant pressure boundary is assumed for the furnace exit.

When we are evaluating the cell face velocities, linear interpolation of the neighboring node values on the non-staggered grid may lead to an oscillatory pressure field (provided that the cell-face peclet number is greater than 2). To eliminate the oscillations with the present non-staggered grid arrangement, a new treatment of the locally linearized convective term [5] was introduced.

$$u_{\mathrm{w}}^{*}=\frac{u_{\mathrm{w}}^{*}+u_{\mathrm{p}}^{*}}{2}-\lambda_{\mathrm{d}}\left\{K_{\mathrm{W}}\frac{\partial f^{\mu}}{\partial\chi}\,|_{\mathrm{W}}-C_{\mathrm{W}}\times\left[\frac{1}{2}\left(\frac{\partial p^{*}}{\partial\chi}\,\Big|_{\mathrm{W}}+\frac{\partial p^{*}}{\partial\chi}\,|_{\mathrm{p}}\right)-\frac{\partial p^{*}}{\partial\chi}\,|_{\mathrm{W}}\right]\right\} \tag{14}$$

where λ_{d} is a scaling factor with typical values of 0.5–1.0, $K_{\mathrm{w}}=\Delta\chi_{\mathrm{w}}/4(V_{\mathrm{P}}/A_{\mathrm{P}}-V_{\mathrm{W}}/A_{\mathrm{w}})$, f^{μ} is the source term from which the pressure gradient term is excluded: $C_{\mathrm{w}}=V_{\mathrm{w}}/a_{\mathrm{w}}$. Variables with subscript 'w' represents those at cell face, while those with majuscule subscript 'W' represents variables at nodes westwards of controlled volume P.

3.3. Turbulent model

The standard k-ε model performs well in predicting flows without swirling flow or without sharp change within the calculated region. But for tangentially fired boiler furnace, where swirling flow is very marked, we must resort to other more valid, more efficient turbulent model to gain accuracy. In this paper, we try to use RNG k-ε model [12] as an alternative substitution for standard k-ε model.

Generally, k and ε equations are follows:

$$u_j\frac{\partial k}{\partial x_j}=P_k-\varepsilon+\frac{\partial}{\partial x_j}\left[\left(v+\frac{v_T}{\sigma_T}\right)\frac{\partial k}{\partial x_j}\right] \tag{15}$$

$$u_j\frac{\partial\varepsilon}{\partial x_j}=C_{\varepsilon1}\frac{\varepsilon}{k}P_K-C_{\varepsilon2}\frac{\varepsilon^2}{k}+\frac{\partial}{\partial x_j}\left[\left(v+\frac{v_T}{\partial_T}\right)\frac{\partial\varepsilon}{\partial x_j}\right] \tag{16}$$

$$P_K=2v_T\overline{S_{ij}S_{ij}},\ \bar{S}_{ij}=\frac{1}{2}\left(\frac{\partial u_i}{\partial x_j}+\frac{\partial u_j}{\partial x_i}\right),\ v_T=C_\mu\frac{k^2}{\varepsilon},$$
$$k=\frac{\overline{u_iu_i}}{2},\ \varepsilon=v\overline{\frac{\partial u_i}{\partial x_j}}\,\overline{\frac{\partial u_i}{\partial x_j}} \tag{17}$$

There are two differences between the two models; one lies in the coefficient:

For standard k-ε model

$$C_\mu=0.09,\ C_{\varepsilon1}=1.44,$$
$$C_{\varepsilon2}=1.42,\ \sigma_K=1.0,\ C_\varepsilon=1.3.$$

For RNG k-ε model

$$C_\mu=0.085,\ C_{\varepsilon1}=1.42-\eta\left(\frac{-\eta/\eta_0}{1+\beta\eta^3}\right),$$
$$C_{\varepsilon2}=1.68,\ \sigma_K=0.7179,\ C_\varepsilon=0.7179,\ \eta=\frac{SK}{\varepsilon},$$
$$S=(2\bar{S}_{ij}\bar{S}_{ij})^{1/2},\ \beta=0.015,\ \eta_0=4.38.$$

The other difference is there is no need to introduce wall function when applying the RNG k-ε model. The introduction of some coefficients in the RNG k-ε model like $C_{\varepsilon1}$ enable it to handle flows with sharp changes within calculated regions. By comparing with experimental data it shows that the RNG k-ε model can give better results for swirling flow and sharp change flow within calculated regions than the standard k-ε model. The detailed discussions on the effects of the two models are included in Section 5.

3.4. A stochastic turbulent particle dispersion model

In an attempt to model turbulent dispersion of particles, we take the stochastic model as recommended by Fan et al. [13].

The instantaneous gas phase velocity

$$u_{\mathrm{f}}=U_{\mathrm{f}}+u_{\mathrm{f}}' \tag{18}$$

in which, U_{f} is the average velocity obtained from the mean velocity field. The fluctuating velocity in an eddy is simulated by means of a random Fourier series

$$u_{\mathrm{g}}'=\sum_{n=1}^{n=10}R_1U_{\mathrm{m}}\cos(\varpi_nt-R_2\alpha) \tag{19}$$

in which R_1, R_2 are random numbers varying between zero and unity, α the initial fluctuating phase, and ϖ_n is sampled from a Gaussian distribution with a standard deviation of unity. For incompressible, isotropic turbulent flow field, the fluctuation amplitude

$$U_{\mathrm{m}}=\left(\int_0^\infty E(K)\,\mathrm{d}K\right)^{1/2} \tag{20}$$

Table 2
Operation cases

Parameters	Load (MW)	Swinging type of burner	OFA
Base case	600	Horizon	–
Case 2	600	Horizon	Cast
Case 3	600	Downswing	–
Case 4	480	Horizon	–

in which, $E(K)$ is the energy spectrum, K is the wave number.

$$E(K) = 16\left(\frac{2}{\pi}\right)^{1/2} K^4 \mathrm{e}^{-2K^2} \tag{21}$$

After completing particle tracing in the furnace, source terms related to momentum, mass transfer, gas reaction heat are obtained, which will then be put back into corresponding equations as ways of coupling. The disadvantage of the Lagrangian/Eulerian approach is that these source terms always appear non-uniform due to probability error. The probability error results from finite particle tracing in the furnace, because of restrict of the amount of calculation, it is impossible to trace infinite particle. An alternate way to reduce the error is to make use of probability theory to average source term curves. In this work, we take advantage of the Weibull probability density function to treat statistically the particle source terms.

3.5. Temperature deviation

Gas temperature deviation, that is, non-uniform gas temperature distribution, has been a long time problem in tangentially fired furnace that sometimes results in pipe explosion of super-heaters and re-heaters. The deviation is supposed to be caused by the inertial effect of the swirling flow, namely, after-swirl that is still significant in the upper furnace. In this work, we take advantage of numerical method to investigate quantitatively the reason for gas temperature deviation, which will be included later.

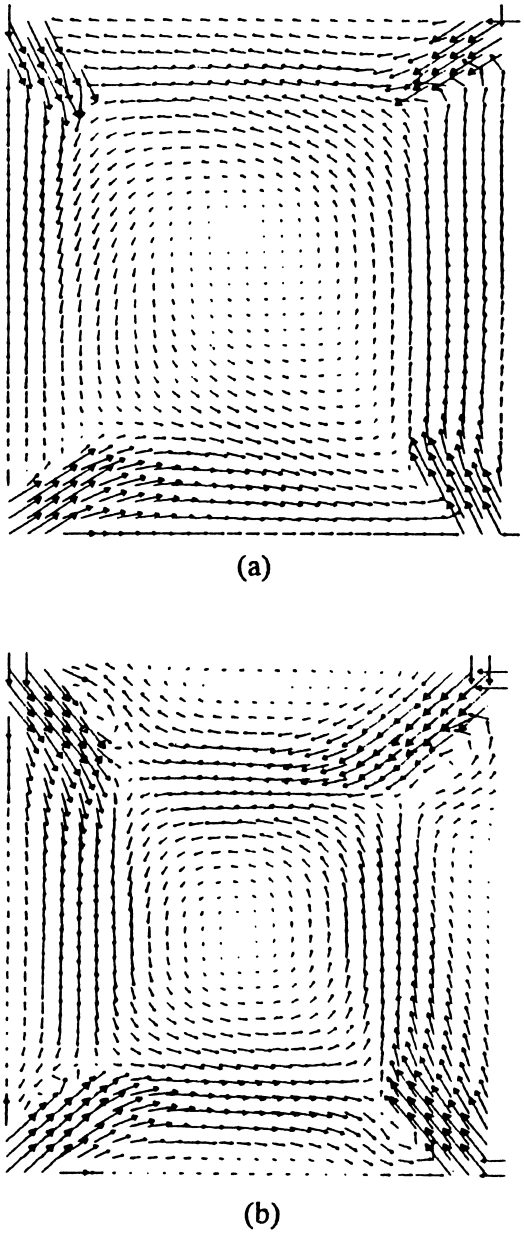

Fig. 1. Flow field: (a) exponential scheme; (b) artificial viscosity method.

4. Numerical algorithms

The model described is applied to a full-scale utility furnace, which is part of a 600 MW tangentially fired utility boiler with 15 level burners. The height of the furnace was 57.075 m. The operating parameters for four cases are listed in Table 2. The analysis of the coal used is presented in Table 3. Using 16 different size classes represents a continuous distribution of coal-particle sizes. The mass fractions for various size classes are shown in Table 4.

Table 3
Analysis of coal used

Proximate analysis (%)				Ultimate analysis (%)					Heating value (MJ/kg)
MS	Ash	VM	FC	C	H	O	N	S	
8.66	24.24	25.36	41.74	53.05	3.86	8.3	1.00	0.89	20.93

The calculation strategy starts with solving the gas flow-field equations assuming that the particles are absent. Using the flow field, particles' trajectories, their temperature and burnout histories are determined. The mass, momentum and energy source terms for each cell is calculated. The source terms are included in the gas-phase equations and the flow field is then recalculated. The process is repeated until

Table 4
The percentages of various size classes of pulverized coal

Particle diameter (μm)	5	20	40	60	80	100	120	140
Percentage	20.22	28.04	17.92	11.61	7.58	4.97	3.27	2.16
Particle diameter (μm)	160	180	200	220	240	260	280	300
Percentage	1.42	0.94	0.62	0.41	0.27	0.18	0.12	0.25

further repetition fails to change the solution. Thus, The mutual interaction of the gas and particles is accounted for. The overall convergence is achieved after about 2500–3500 iterations.

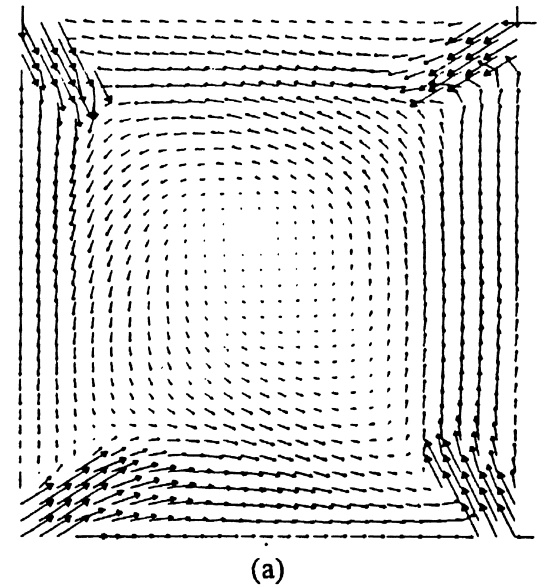

Fig. 2. Grid-independence tests: (a) grid comprising 35×37×143; (b) grid comprising 40×45×155.

5. Results and discussions

Fig. 1 shows the predicted results of flow filed on a cross-section. Fig. 1(a) is the results using the exponential scheme, while Fig. 1(b) is the results using the artificial viscosity method. After comparison, we can see from Fig. 1(a) gas flow poses very skewed distribution and appears to be not uniform due to over-diffusion at some places, which renders gas velocity near the wall as non-zero, while Fig. 1(b) gives a more uniform and seemingly more reasonable results by artificial control of pseudo-diffusion. In order to improve the stability of calculation, the artificial viscosity method should be written into an implicit form. Actually, solution to equations with artificial viscosity is approaching the precise solution for the one-dimension convection-diffusion Eq. [9].

Fig. 2 shows the result of grid-independence tests. Fig. 2(a) uses a grid comprising 35×37×143, Fig. 2(b) uses a grid comprising 40×45×155. Because of the restrict of the amount of calculation and time, it is impossible to use much bigger grid than it that we are using now. Though we can find there are numerical errors to a certain degree from the figure, it is permitted. So we can conclude that the specified grid is fine enough to give grid-independent solution.

Fig. 3 shows *x*-direction velocity on the *x*-direction centerline and *y*-direction velocity on the *y*-direction centerline at some combustor cross-section. We compare results by using standard *k*-*ε* and RNG *k*-*ε* models, respectively. We have experimental data that are taken at the cross-section at the height of one of secondary combustors to compare. As shown in Fig. 3, the RNG *k*-*ε* model is closer to the experi-

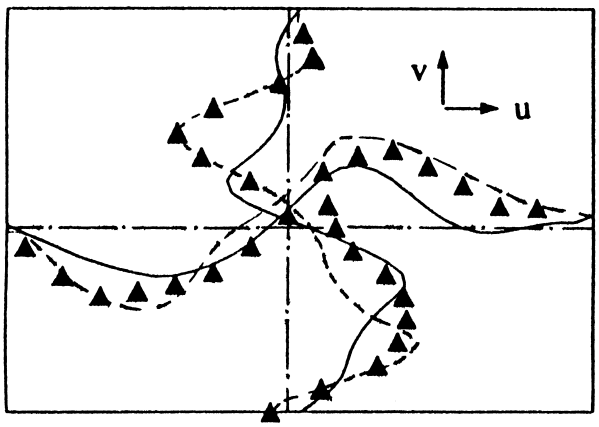

Fig. 3. Velocity profiles on cross-section: (------) RNG *k*-*ε* model; (—) standard *k*-*ε* model; (▲) experiment.

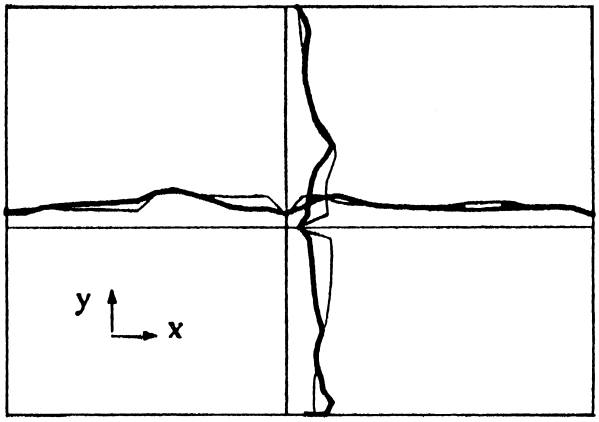

Fig. 4. Turbulent kinetic energy profiles on cross-section: (▬) RNG k-ε model; (—) standard k-ε model.

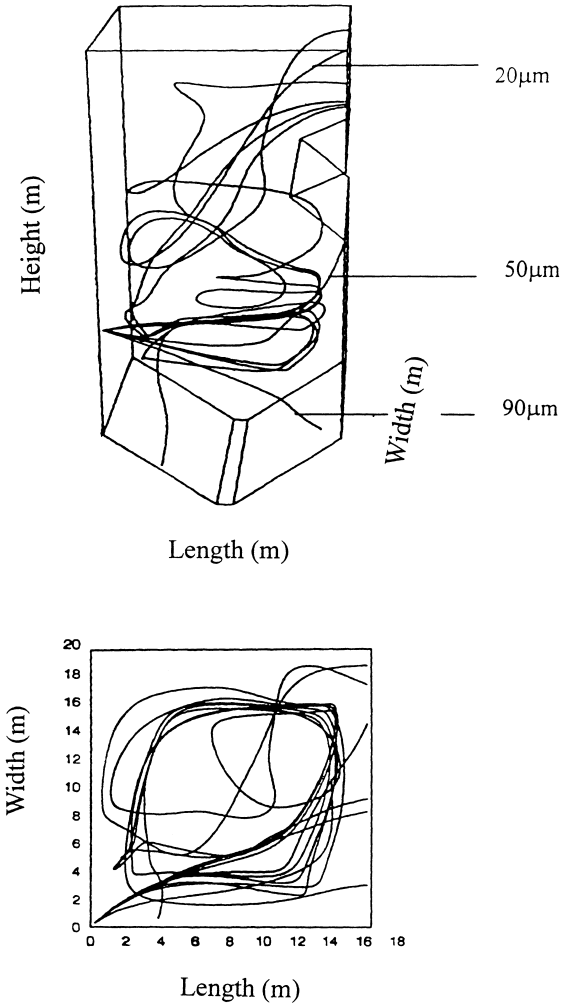

Fig. 5. Trajectories of particles.

mental data than the standard k-ε model, showing the advantage of the former over the latter in treating this kind of swirling flow field. Fig. 4 gives the fluctuating kinetic energy along the x and y-direction centerlines at some combustor cross-section in which one can see that RNG k-ε gives a relatively flatter fluctuating kinetic energy curve. The standard Turbulence k-ε Models have well documented weaknesses in relation to complex flows, so we take the improved agreement with respect to the RNG k-ε model. By comparing with experimental data it shows that the RNG k-ε model can give better results for swirling flow and sharp change flow within calculated regions than the standard k-ε model, so it is meaningful to a certain degree.

Fig. 5 gives several typical particles three-dimensional trajectories after applying the stochastic turbulent diffusion model; the diameters are 20, 50, 90 μm, respectively. The results are reasonably good.

Figs. 6 and 7 show the effects of the Weibull probability function treatment in the source terms of CO, Vr (volatile matter), the two figures are taken at the central y-direction cross-section. By using Weibull's probability density function treatment for source terms, probability errors in source terms are satisfyingly reduced.

Figs. 8–11 that they belong to case 1, 2, 3 and 4, respectively, are temperature comparison between numerical calculation and experimental measurement near the convective superheated tube at the cross-section of the furnace outlet. The place measured lies on the reheated tube nearby outside the furnace, which is 1.5 m away from the

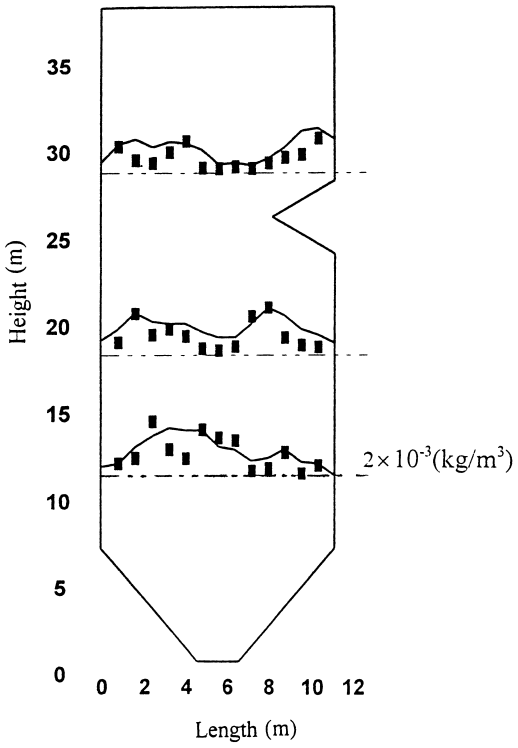

Fig. 6. Source term of CO (kg/m^3): (▮) source term before Weibull treatment; (—) source term after Weibull treatment.

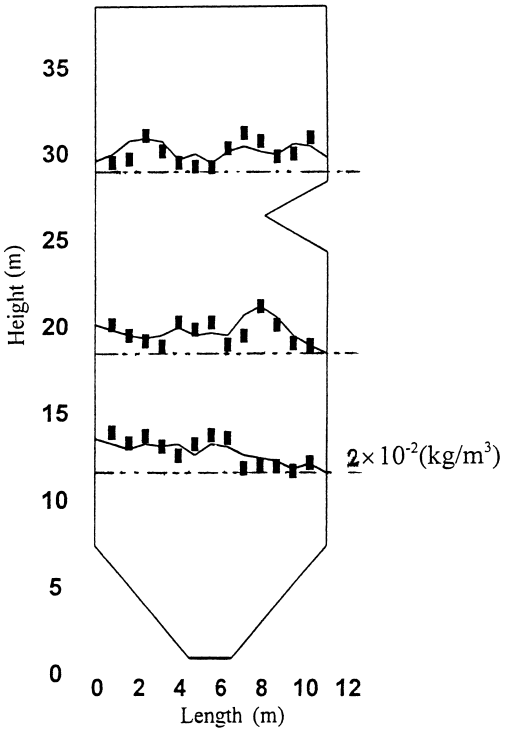

Fig. 7. Source term of Vr (kg/m^3): (▮) source term before Weibull treatment; (—) source term after Weibull treatment.

boiler'top wall. The calculated result has some fluctuation, the fluctuation mainly result from that cell volume size is not enough small and discrete energy number for each cell in the furnace is not so much. Because of the restrict of the amount of calculation and time, it is impossible to trace infinite discrete energy and use too small cell volume size in the furnace, but the result calculated has the same trend roughly as the experimental data. The boiler had been rebuild before we calculated it, so the temperature deviation is not very obvious. Because non-uniform velocity results in non-uniform heat-absorption, the temperature deviation results from non-uniform velocity. The non-uniform velocity actually results from the survival after-swirl of the furnace

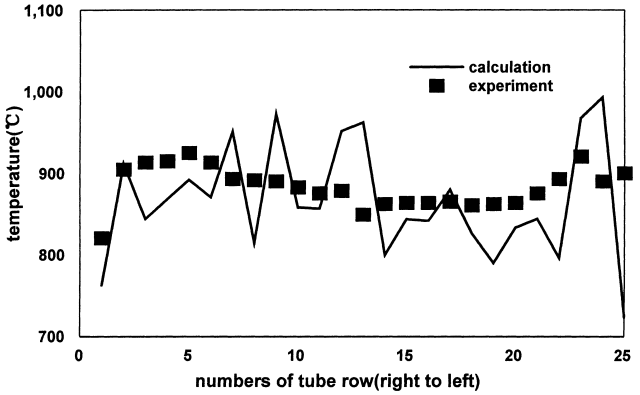

Fig. 8. Flue gas temperature of near the super-heater at aclinic flue (case 1).

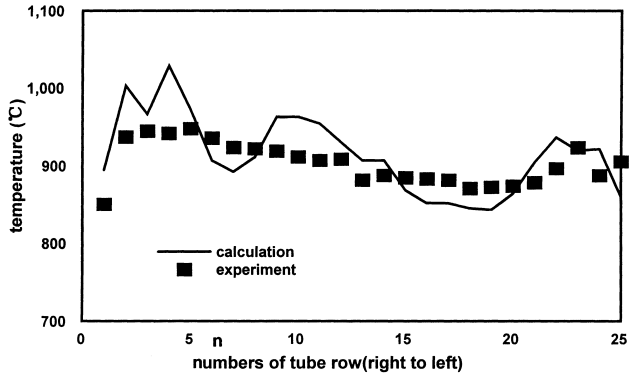

Fig. 9. Flue gas temperature of near the super-heater at aclinic flue (case 2).

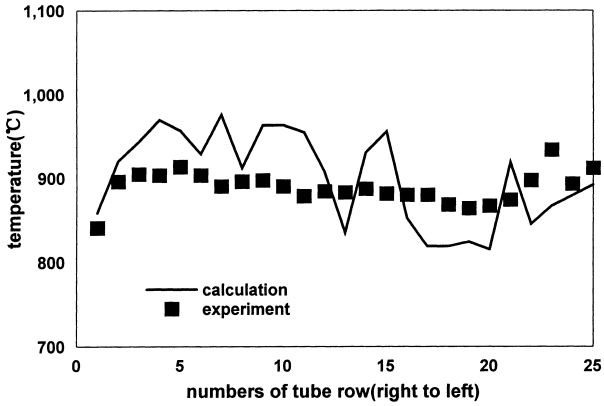

Fig. 10. Flue gas temperature of near the super-heater at aclinic flue (case 3).

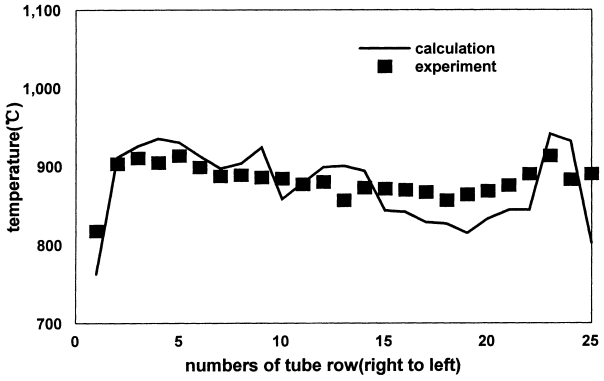

Fig. 11. Flue gas temperature of near the super-heater at aclinic flue (case 4).

outlet, so after-swirl is the one that is to take the blame for the temperature deviation.

6. Conclusions

We have made several attempts at improving accuracy in simulating combustion processes inside tangentially fired furnaces. To gain a reasonably good prediction of the aero-

dynamic field, we made comparisons between the exponential scheme and an artificial method, and then between standard k-ε and RNG k-ε models. We found that the artificial viscosity method and the RNG k-ε model can to some degree give a relatively accurate prediction. We also introduce a stochastic turbulent diffusion model into particle tracing and then Weibull's method to reduce probability error in source terms. We analyze what causes temperature deviation. The ultimate reason lies in non-uniform gas velocity distribution that is the innate drawback of the tangentially fired boiler. The data resulting from the present study may be used to enhance the understanding of combustion processes and also provide a useful basis for further researching comprehensive models of combustion processes and designing and operating boiler furnaces with high-efficiency.

Acknowledgements

Supported by the special funds of Major State Basic National Importance Foundation Research Projects of PR China.

References

[1] F.C. Lockwood, C. Papadopoulos, A.S. Abbs, Prediction of corner-fired power station combustor, Combust. Sci. Technol. 58 (1988) 5–23.

[2] K.L. Simth, S.C. Hill, L.D. Smoot, Theory for NO formation in turbulent coal flames, in: Proceedings of the 19th International Symposium on Combustion, The Combustion Institute, Pittsburgh, PA, 1982, pp. 1263–1269.

[3] L.D. Smoot, Modeling of coal-combustion processes, Proc. Energy Combust. Sci. Technol. 10 (1984) 229–272.

[4] J.R Fan, X.H. Liang, Q.S. Xu, X.Y. Zhang, K.F. Cen, Numerical simulation of the flow and combustion process in a three-dimensional, W-shaped boiler furnace, Energy 22 (1997) 847–857.

[5] M.M. Rahman, A. Miettinen, T. Siikonen, Modified simple formulation on a collocated grid with an assessment of the simplified quick scheme, Numerical Heat Transfer Part B 30 (1996) 291–314.

[6] W.B. Fu, Y.P. Zhang, H.G. Han, Y.N. Duan, Combust. Flame 70 (1987) 253.

[7] J.R. Fan, X.H. Liang, Q.S. Xu, X.Y Zhang, K.F. Cen, Numerical simulation of the flow and combustion processes in a three-dimensional, W-shaped boiler furnace, Energy 8 (1997) 847–857.

[8] S.V. Patankar, D.B. Spalding, Int. J. Heat Mass Transfer 15 (1972) 15 1987.

[9] Y.R. Fan, A.L. Ren, A study on pseudo-diffusion of the numerical simulation of cold flow in tangentially fired furnace, in: Proceedings of the Second International Symposium on Coal Combustion, Peking, 1991, pp. 224–229.

[10] J.R. Fan, X.H. Liang, Q.S. Xu, X.Y. Zhang, K.F. Cen, Numerical simulation of the flow and combustion process in a three-dimensional, W-shaped boiler furnace, Energy 22 (1997) 847–857.

[11] J.S.M. Botterill, Fluidized Bed Heat Transfer, Academic Press, London, 1975.

[12] V. Yakhot, S.A. Orszag, Renormalization group analysis of turbulence, J. Sci. Comput. 1 (1986) 39–51.

[13] J.R. Fan, X.Y. Zhang, L.H. Chen, K.F. Cen, New stochastic particle dispersion modeling of a turbulent particle-laden round jet, Chem. Eng. J. 66, 207–215.